Progress In Electromagnetics Research, Vol. 127, 461–478, 2012

PRINCIPLE COMPONENT ANALYSIS AND FUZZY LOGIC BASED THROUGH WALL IMAGE ENHANCEMENT

M. M. Riaz and A. Ghafoor*

Department of Electrical Engineering, College of Signals, National University of Sciences and Technology (NUST), Islamabad, Pakistan

Abstract—Principle component analysis based through wall image enhancement is proposed which is capable of discriminating target, noise and clutter signals. The overlapping boundaries of clutter, noise and target signals are separated using fuzzy logic. Fuzzy inference engine is used to assign weights to principle components. The proposed scheme works well significantly for extracting multiple targets having different range profiles in heavy cluttered through wall images. Simulation results are compared on the basis of mean square error, peak signal to noise ratio and visual inspection.

1. INTRODUCTION

Through Wall Imaging (TWI) is an active research area due to its wide range of applications (especially in rescue, military, surveillance and remote sensing). TWI (seeing through opaque materials) gives the ability to examine building structure layout, detection and localization of target(s). Compared to other remote sensing techniques (ground penetrating radar and medical imaging), TWI has to deal with variety of challenges (propagation environment, sensor positioning and operational requirements). Moreover, propagation medium (often composed of multiple unknown, non-homogenous and non-uniform walls) leads to multi-paths and strong clutters which makes TWI a complex and challenging problem [1].

TWI system works on synthetic aperture RADAR principle. Electromagnetic pulse of certain frequency is transmitted that reflects from target and is received with some attenuation [2]. Low frequencies

Received 27 January 2012, Accepted 26 April 2012, Scheduled 3 May 2012

* Corresponding author: Abdul Ghafoor (abdulghafoor-mcs@nust.edu.pk).

provide good penetration through walls but result in poor resolution compared to high frequencies. However, antennas become large at low frequencies which restrict lower frequency range to 1 GHz practically. On the other hand, if we address detection through concrete walls, the upper frequency range is limited to 3 GHz [3].

Hardware setup (antennas, Vector Network Analyzer (VNA) and position controller) and software algorithms for TWI are improving day by day [4]. Once the hardware receive the reflected signals, the first task is to reconstruct image by measuring attenuation coefficient and total flight time. Various methods of image reconstruction in TWI include Kirchhoff migration, f-k migration, differential SAR and beamforming, etc. [4]. Improvements [4–13] are suggested to overcome some limitations (like knowledge of wall parameters, incidence and reflective angles, homogenous medium, multiple targets and point target, etc.). Reconstructed image quality directly affects the target classification accuracy.

Image enhancement in TWI, has enjoyed an increasing interest over last few years [14–27]. Clutter and noise (due to antenna attenuation, cross talk, false targets and wall reflections) result in degradation of image quality, ambiguity in localization of targets and appearance of false targets. Techniques for image enhancement in TWI include, background subtraction [14], spatial filtering [15], wall parameter estimation/modeling based [17, 18], doppler domain filtering [21], image fusion [22, 23] and statical methods.

Major drawback of background subtraction technique is that it requires a surveillance mode of operation in which there is an access to the background (image scene that is free from targets) or reference [14, 20]. Spatial filtering relies on invariance of wall characteristic (where wall return remains same with changing antenna location). Moreover, this scheme works only for homogeneous (or near-homogeneous) walls at low operating frequencies [15, 20]. Limitation of wall parameter estimation/modeling based approach is that it requires accurate modeling and parameter estimation [17, 20]. Doppler domain filtering assumes that background is stationary and targets are moving so a doppler shift occurs which can be used to discriminate target and clutter signals [21]. Image fusion methods require multiple images of same scene from different locations (which is not possible especially in case of moving targets) [22, 23]. Some statistical method for TWI enhancement include Singular Value Decomposition (SVD), Factor Analysis (FA), Principal Component Analysis (PCA) and Independent Component Analysis (ICA) [27]. Statistical methods having less computational complexity and provide comparable results to other image enhancement methods. However these methods (SVD, PCA,

FA and ICA) suffer from limitation that total number of targets are known a-priori. Statistical methods sometimes also require a subjective threshold value.

PCA and fuzzy logic based image enhancement is proposed for TWI which provides better accuracy than existing PCA based image enhancement. PCA is chosen for its low complexity and simplicity over other methods (SVD, FA and ICA). Proposed method successfully estimates total number of targets and result in improved image quality. Proposed scheme significantly works well for extracting multiple targets in heavy cluttered TWI image. Existing and proposed algorithms are compared on the basis of mean square error, peak signal to noise ratio and visual inspection.

2. IMAGE ENHANCEMENT

2.1. Data Acquisition and Image Reconstruction

TWI setup is shown in Figure 1 while geometrical representation of TWI is shown in Figure 2.

Let H transceivers be placed (parallel to the x-axis) in the x-y plane. Image region (located beyond the wall along the positive y-axis) is divided into grid of $M \times N$ pixels ($m = 1, 2, 3 \ldots, M$ and $n = 1, 2, 3 \ldots, N$). Let $\theta(t)$ be a wideband transmitted signal then pixel value at location mn can be computed by weighted sum and delay beamforming [4]. Output $\zeta_{mn}(t)$ for target located in x-y plane

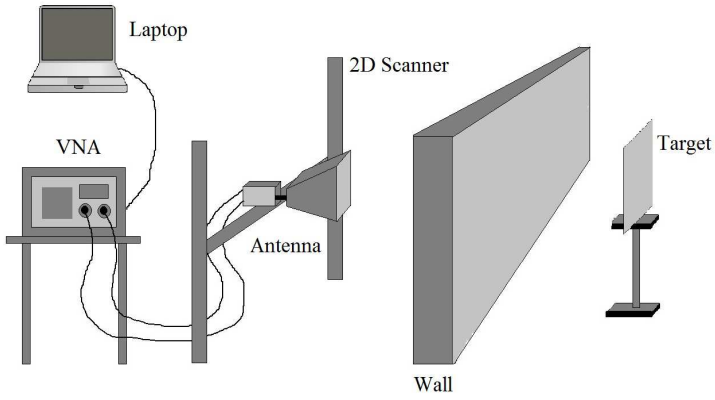

Figure 1. TWI setup.

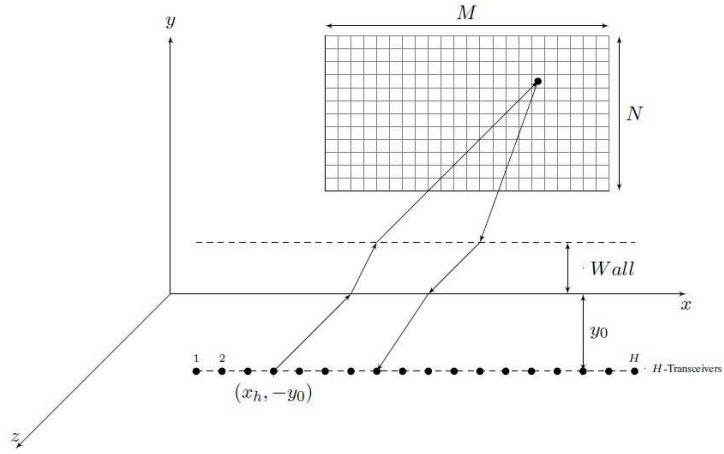

Figure 2. Geometrical representation of TWI.

at pixel location mn is given by:

$$\zeta_{mn}(t) = \sum_{p,q}^{H} \xi(p,q)\vartheta(t + \tau_{mn}(p,q))$$

where $\xi(p,q)$ are weights (normally based on Kaiser or Hamming window) used to control side lobes, and $\tau_{mn}(p,q)$ is time delay. Received signal $\vartheta(t)$ is delayed version of transmitted signal $\theta(t)$ with some attenuation $\alpha_{mn}(p,q)$, i.e., $\vartheta_{mn}(t) = \alpha_{mn}(p,q)\theta(t - \tau_{mn}(p,q))$ where $\tau_{mn}(p,q)$ are time delays. Let $\hat{\theta}(t) = \theta(-t)$ be a filter matched to transmitted signal then the de-convoluted output for pixel mn, f_{mn} is given as:

$$f_{mn} = \left(\zeta_{mn}(t) * \hat{\theta}(t)\right)\Big|_{t=0}$$

$$f_{mn} = \left(\sum_{p,q}^{H} \alpha_{mn}(p,q)\xi(p,q)\theta(t - \hat{\tau}_{mn}(p,q) + \tau_{mn}(p,q)) * \hat{\theta}(t)\right)\Bigg|_{t=0}$$

$\hat{\tau}_{mn}(p,q)$ are estimated time delays and can be calculated by various methods depending on the available wall information [2]. Above process is repeated for each pixel location mn to obtain B-scan image.

$$F = \begin{pmatrix} f_{11} & f_{12} & \cdots & f_{1N} \\ f_{22} & f_{22} & \cdots & f_{2N} \\ \vdots & \vdots & \ddots & \vdots \\ f_{M1} & f_{M2} & \cdots & f_{MN} \end{pmatrix}$$

2.2. PCA Based Image Enhancement

PCA transforms correlated variables into a set of uncorrelated variables called principal components. First principal component has highest variance and succeeding components have as high variance as possible under the constraint that it will be orthogonal to the preceding components. PCA (also named as discrete Karhunen Loeve transform, Hotelling transform and proper orthogonal decomposition) is used in variety of data analysis applications (dimension reduction of complex data sets, noise reduction and probability density function estimation) ranging from neuroscience to computer graphics because of its simplicity and non-parametric method of extracting relevant information from confusing data sets [28, 29]. Image enhancement in TWI can be performed by decomposing B-scan image into different spectral components (subspaces). Let B-scan image F be composed of target S and noise V images.

$$F = S + V$$

Covariance matrix C_F of image F is:

$$C_F = \frac{1}{N} F F^T = C_S + \sigma_V^2 I \tag{1}$$

where noise is modeled as white noise having variance σ_V^2, C_S is covariance matrix of targets and I is identity matrix. C_F is decomposed into different spectral components using eigen value decomposition, i.e.,

$$C_F = \Gamma \Lambda_S \Gamma^T + \sigma_V^2 I = \Gamma(\Lambda_S + \sigma_V^2)\Gamma^T = \Gamma \Lambda \Gamma^T = \sum_{m=1}^{M} \lambda_m \gamma_m \gamma_m^T$$

where Γ is $M \times M$ unitary matrix ($\Gamma^{-1} = \Gamma^T$) containing eigen vectors $\Gamma = [\gamma_1 \ \gamma_2 \ \ldots \ \gamma_M]$, Λ is diagonal matrix containing eigen values, i.e., $\Lambda = \Lambda_S + \sigma_V^2 I = \mathrm{diag}[\lambda_1 \ \lambda_2 \ \ldots \ \lambda_M]$, $\lambda_i = \lambda_{s_i} + \sigma_V^2$ and $\lambda_1 \geq \lambda_2 \geq \ldots \geq \lambda_M$. Principle components matrix $\Phi = [\phi_1 \ \phi_2 \ \ldots \ \phi_M]$ is:

$$\Phi = F^T \Gamma \tag{2}$$

$F = \Gamma \Phi^T$ can be decomposed into different subspaces as:

$$F = \sum_{m=1}^{M} \gamma_m \phi_m^T = \sum_{m=1}^{k_1} \gamma_m \phi_m^T + \sum_{m=k_1+1}^{k_2} \gamma_m \phi_m^T + \sum_{m=k_2+1}^{M} \gamma_m \phi_m^T$$

where first k_1 principle images belong to wall clutters followed by k_2 target images and the rest are noise images. Above statement is derived from the fact that when eigen value belong to target then

$\lambda_m = \lambda_{s_m} + \sigma_V^2 \simeq \lambda_{s_m}$ because $\lambda_{s_m} \gg \sigma_V^2$ and incase when eigen value does not belong to target $\lambda_m = \lambda_{s_m} + \sigma_V^2 \simeq \sigma_V^2$ because $\lambda_{s_m} \ll \sigma_V^2$. It is observed that difference between noise eigenvalues $\Delta\lambda_m = \lambda_m - \lambda_{m+1}$ are relatively small than target eigenvalues. Verma, et al. in [4] state that $k_1 = 1$ for wall clutter and $k_2 = 2$ for target subspaces and rest subspaces represent noise. However, we note that this statement (by Verma, et al.) is not true in case of multiple targets. We observe that number of targets (which are not known a-priori) determine the value for k_2. Therefore, some statistical analysis needs to be performed in order to determine value for k_2. In this regard, some schemes are found in literature like difference of eigen values $(\lambda_m - \lambda_{m+1})$, ratio of eigen values $(\lambda_m/\lambda_{m+1})$ and percent of total power in an eigen value $(\lambda_m/tr[C_F])$. These methods do not always provide satisfactory results (and some times require a user defined threshold).

2.3. PCA and Fuzzy Logic Based Image Enhancement

It is observed that the boundaries of clutter, noise and target signals are not sharply defined. Therefore, it is not possible to extract target eigen values accurately. This motivates use of weights to sharpen the boundaries of clutter, noise and target signals. It is observed that when λ_m and $\Delta\lambda_m$ are high, then λ_m possibly belongs to target and need to be enhanced by applying heavy weights. Otherwise λ_m belongs to noise and clutter and needs to be suppressed by assigning light weights. Figure 3 describe this concept.

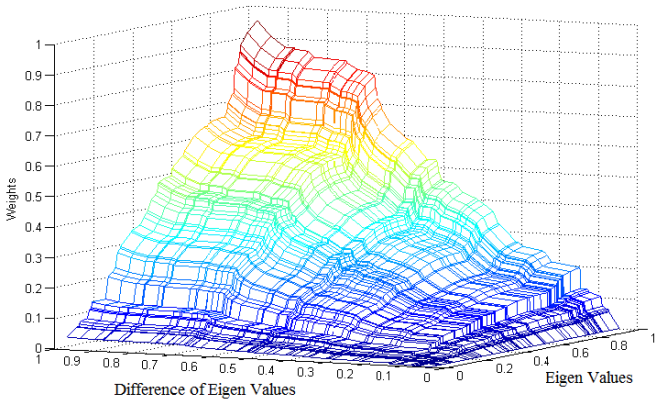

Figure 3. Illustration of weighted PCA.

Let ϖ_m be weight assigned to mth principle component:

$$F_{tar} = \sum_{m=2}^{M} F_m \varpi_m = \sum_{m=2}^{M} \gamma_m \phi_m^T \varpi_m \tag{3}$$

Various weight assignment techniques like linearly weights, exponentially weights, logistic weights, fuzzy weights, etc.) are available in literature but are never explored (to the best of authors's knowledge) for TWI image enhancement. Some weighting schemes are defined as:

- Linear weights

$$\varpi_m = \frac{\psi_1 \lambda_m + \psi_2 \Delta\lambda_m}{\psi_3} \tag{4}$$

- Exponential weights

$$\varpi_m = \frac{e^{(\psi_1 \lambda_m + \psi_2 \Delta\lambda_m)}}{\psi_3} \tag{5}$$

- Logistic weights

$$\varpi_m = \frac{\psi_3}{1 + e^{-}(\psi_1 \lambda_m + \psi_2 \Delta\lambda_m)} \tag{6}$$

where ψ_1 and ψ_2 are constants used to control the effect of λ_m and $\Delta\lambda_m$ respectively and ψ_3 is normalizing constant. Above weight assignment techniques appear simple to use but their main drawback is empirical determination of constants (ψ_1,ψ_2 and ψ_3) are empirical. Note that, weight assignment using fuzzy logic is automatic therefore we use it for TWI image enhancement.

Figure 4 shows block diagram of a fuzzy system.

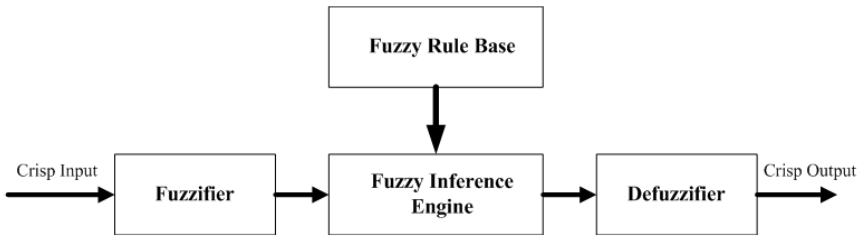

Figure 4. Fuzzy system.

2.3.1. Gaussian Fuzzifier (GF)

Let eigen values λ_m and difference of eigen values $\Delta\lambda_m$ can be represented in vector notation as below:

$$\mathbf{x}^* = [x_1^* \quad x_2^*] = [\lambda_m \quad \Delta\lambda_m]$$

where $\mathbf{x}^* \in R^2$ represents real value points. We define gaussian membership functions $\mu_{A^d}(x_1)$ and $\mu_{B^e}(x_2)$ for inputs as under:

$$\mu_{A^d}(x_1) = e^{-\left(\frac{x_1-\bar{x}_1^{(d)}}{\sigma_1^{(d)}}\right)^2} \tag{7}$$

$$\mu_{B^e}(x_2) = e^{-\left(\frac{x_2-\bar{x}_2^{(e)}}{\sigma_2^{(e)}}\right)^2} \tag{8}$$

where $d = 1, 2, 3$ and $e = 1, 2, 3$ represents number of fuzzy sets. $\bar{x}_1^{(d)}$, $\bar{x}_2^{(e)}$ and $\sigma_1^{(d)}$, $\sigma_2^{(e)}$ are constant parameters representing means and variances of fuzzy sets. GF is used to map $\mathbf{x}^* \in R^2$ into fuzzy set AB having following gaussian membership function:

$$\mu_{AB}(x_1, x_2) = e^{-\left(\frac{x_1-x_1^*}{a_1}\right)^2} \star e^{-\left(\frac{x_2-x_2^*}{a_2}\right)^2} = e^{-\left(\frac{x_1-x_1^*}{a_1}\right)^2} e^{-\left(\frac{x_2-x_2^*}{a_2}\right)^2} \tag{9}$$

where $\star$ is t-norm operator and is taken as algebraic product. a_1 and a_2 are positive parameters used for noise suppression in input data (e.g., if a_1 and a_2 are larger than $\sigma_1^{(d)}$, $\sigma_2^{(e)}$ the noise will be greatly suppressed so one can choose $a_1 = 2 \max_{d=1}^{3} \sigma_1^{(d)}$ and $a_2 = 2 \max_{e=1}^{3} \sigma_2^{(e)}$. GF has the advantage over other fuzzifiers in terms of accuracy [30, 31].

2.3.2. Product Inference Engine (PIE)

PIE process fuzzy inputs based on fuzzy rule base and linguistic rules. PIE structure consists of individual rule based inference with union combination, Mamdani product implication, algebraic product for t-norm and max operator for s-norm [31]. Fuzzy IF-THEN rules for noise and clutter reduction are defined on experimental observations that the eigen values of target signals have high magnitude and spread compared to noise signals. Fuzzy rule-base decision matrix for image enhancement is shown in Figure 5.

$Ru^{(1)}$: If λ_m is A^1 and $\Delta\lambda_m$ is B^1 then y_m is C^1.

$Ru^{(2)}$: If λ_m is A^1 and $\Delta\lambda_m$ is B^2 then y_m is C^2.

$Ru^{(3)}$: If λ_m is A^1 and $\Delta\lambda_m$ is B^3 then y_m is C^3.

$Ru^{(4)}$: If λ_m is A^2 and $\Delta\lambda_m$ is B^1 then y_m is C^2.

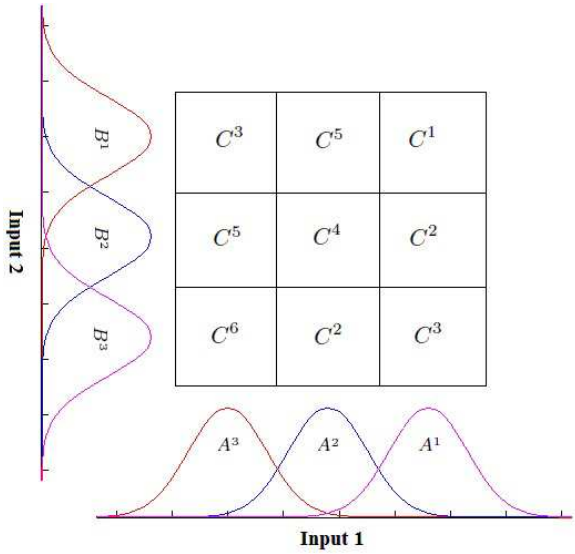

Figure 5. Decision matrix.

$Ru^{(5)}$: If λ_m is A^2 and $\Delta\lambda_m$ is B^2 then y_m is C^4.
$Ru^{(6)}$: If λ_m is A^2 and $\Delta\lambda_m$ is B^3 then y_m is C^5.
$Ru^{(7)}$: If λ_m is A^3 and $\Delta\lambda_m$ is B^1 then y_m is C^2.
$Ru^{(8)}$: If λ_m is A^3 and $\Delta\lambda_m$ is B^2 then y_m is C^5.
$Ru^{(9)}$: If λ_m is A^3 and $\Delta\lambda_m$ is B^3 then y_m is C^6.

C^c for $c = 1, 2, \ldots, 6$ are output membership functions. A^1, A^2, A^3 and B^1, B^2, B^3 are input fuzzy membership functions corresponds to high, medium and low. Similarly C^c are output membership functions with C^1 corresponds to highest and C^6 corresponds to lowest.

$$\mu_{C^c}(y_m) = e^{-\left(\frac{y_m - \bar{y}^{(c)}}{\varrho^{(c)}}\right)^2} \tag{10}$$

where $\bar{y}^{(c)}$ and $\varrho^{(c)}$ are constant parameters representing mean and variances of output fuzzy sets. PIE is defined as:

$$\mu_{C'}(y_m) = \max_{\{c,d,e\}} \left[\sup_{\{x_1,x_2\}} \mu_{AB}(x_1, x_2)\mu_{A^d}(x_1)\mu_{B^e}(x_2)\mu_{C^c}(y_m) \right]$$

Putting values of $\mu_{AB}(x_1, x_2)$, $\mu_{A^d}(x_1)$, $\mu_{B^e}(x_2)$, $\mu_{C^c}(y_m)$, above

equation reduces to:

$$\mu_{C'}(y_m) = \max_{\{c,d,e\}}\left[\exp\left[-\left(\frac{x_1-\bar{x}_1^{(d)}}{\sigma_1^{(d)}}\right)^2-\left(\frac{x_2-\bar{x}_2^{(e)}}{\sigma_2^{(e)}}\right)^2-\left(\frac{x_{1T}^d-\bar{x}_1^d}{a_1}\right)^2 -\left(\frac{x_{2T}^e-\bar{x}_2^e}{a_2}\right)^2\right]\mu_{C^c}(y_m)\right]$$

where,

$$x_{1T}^d=\frac{a_1^2\bar{x}_1^d+(\sigma_1^d)^2x_1^*}{a_1^2+(\sigma_1^d)^2} \quad \text{and} \quad x_{2T}^e=\frac{a_2^2\bar{x}_2^e+(\sigma_2^e)^2x_2^*}{a_2^2+(\sigma_2^e)^2}$$

2.3.3. Center Average Defuzzifier (CAD)

Fuzzy outputs are converted to real world outputs using defuzzification process. CAD specifies the real output y_m^* as the weighted sum of 6 output fuzzy sets having centers $\bar{y}^{(c)}$ and height $w_m^{(c)}$.

$$\varpi_m = y_m^* = \frac{\sum_{c=1}^{6}\bar{y}^{(c)}w_m^{(c)}}{\sum_{c=1}^{6}w_m^{(c)}}$$

CAD has less computational complexity, higher accuracy and continuity than other defuzzifiers (center of gravity, maximum defuzzifier, etc.) [31].

2.3.4. Fuzzy Parameters Selection

For designing a fuzzy system fuzzy parameters selection ($\bar{x}_1^{(d)}$, $\sigma_1^{(d)}$, $\bar{x}_2^{(e)}$, $\sigma_2^{(e)}$ and $\bar{y}^{(c)}$, $\varrho^{(c)}$) is important. For fuzzy sets $x_1 \in [0,1]$, $x_2 \in [0,1]$ and $y \in [0,1]$ one way is to assign uniform spaced membership functions between zero and one as shown in Figure 6. Although this approach is quite simple in nature but it leads to poor results so a novel method based on K-means algorithm is proposed for estimating optimal fuzzy parameters.

K-means [32] is one of the simplest unsupervised data clustering algorithm that classify data into certain number (fixed a priori) of clusters. K-means has applications in various other fields ranging from market segmentation, computer vision, geo-statistics, astronomy and agriculture.

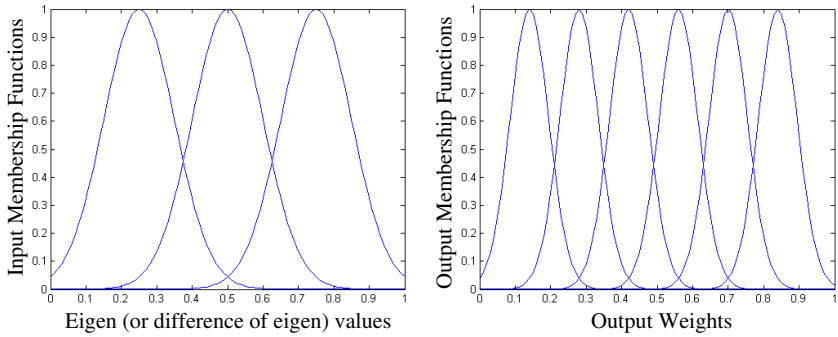

Figure 6. Uniform input and output membership functions. (a) Input. (b) Output.

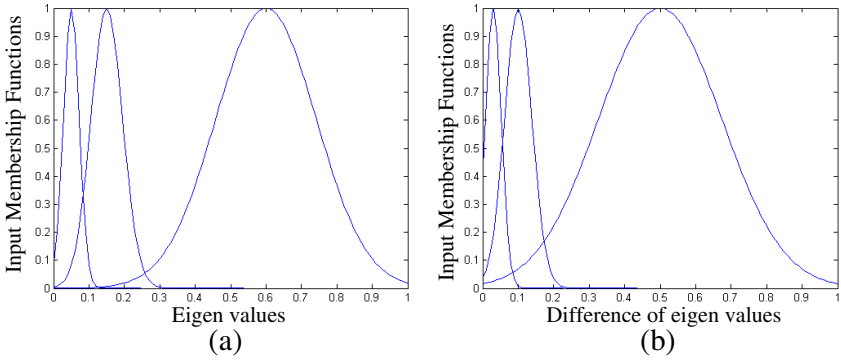

Figure 7. Input membership functions obtained by K-means. (a) Eigen values. (b) Difference of eigen values.

- **Step 1:** Initialize k centroids, i.e., one for each cluster. These centroids should be initialized in a cunning way because different initialization leads different result. Better choice is to place them randomly as far as possible from each other.
- **Step 2:** Assign class labels to data points by using some distance metric (usually euclidian distance is used).
- **Step 3:** Calculate mean (average value) of each class and assign means as new centriods. Repeat Step 2 until change between new and old centriods becomes negligible.

Once data is clustered the centers $\bar{x}_1^{(d)}$, $\bar{x}_2^{(e)}$ and spread $\sigma_1^{(d)}$, $\sigma_2^{(e)}$ are calculated by mean and variance of that class as shown in Figure 7.

As output distribution is not known a-priori so we have used equally spaced output membership functions (as discussed earlier). K-means is sensitive to initial randomly selected centers so the algorithm is run multiple times (with different starting points) to get optimized clustering results.

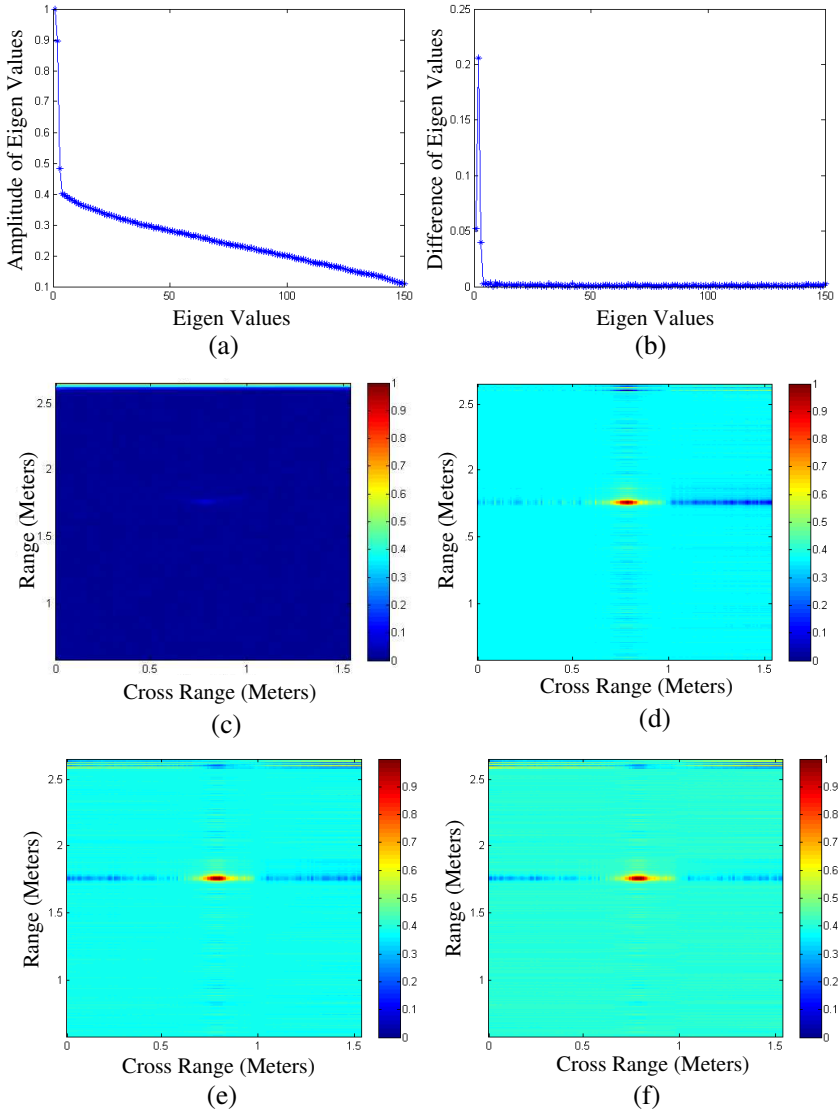

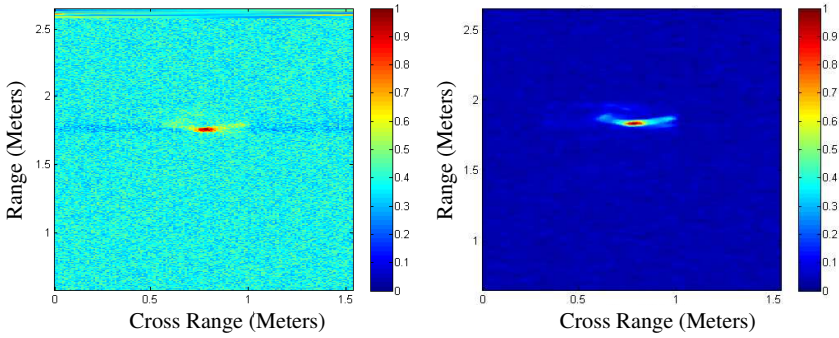

Figure 8. Single target. (a) Eigen values. (b) Difference of eigen values. (c) Original image. (d) Conventional PCA. (e) Fuzzy PCA with uniform membership functions. (f) Fuzzy PCA with K-means based membership functions. (g) Unity weights PCA. (h) Background subtracted image.

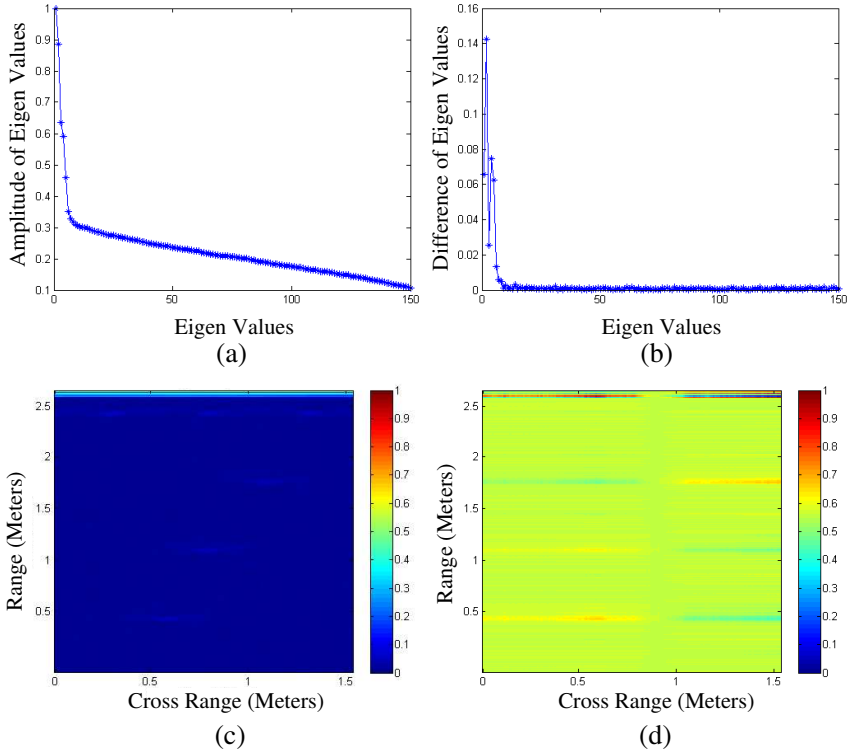

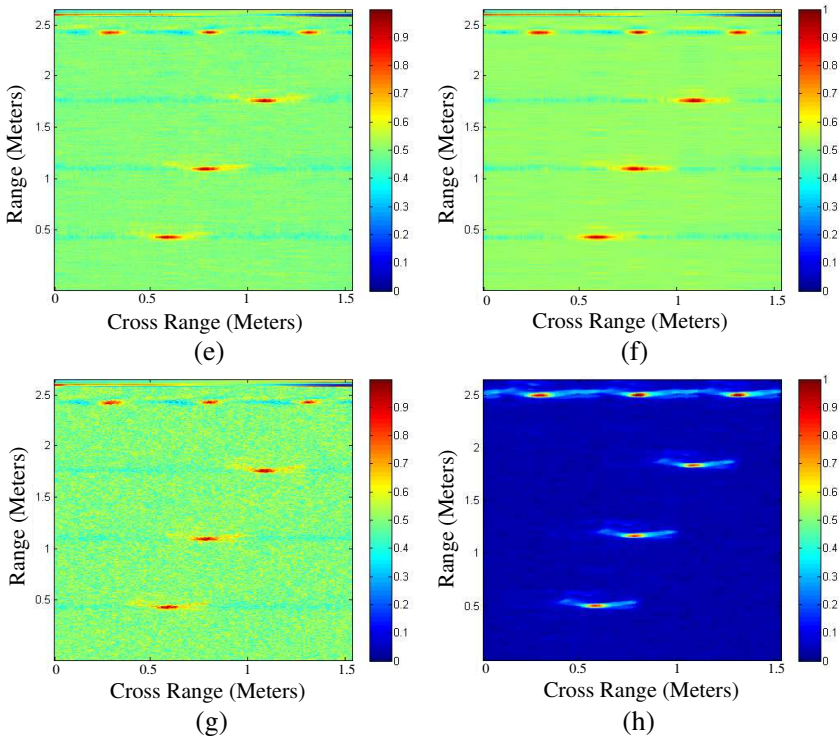

Figure 9. Multiple target. (a) Eigen values. (b) Difference of eigen values. (c) Original image. (d) Conventional PCA. (e) Fuzzy PCA with uniform membership functions. (f) Fuzzy PCA with K-means based membership functions. (g) Unity weights PCA. (h) Background subtracted image.

3. SIMULATION AND RESULTS

Variety of experiments are conducted by varying parameters like type of walls, number and shape of targets and target locations. Experimental setup for TWI consists of Vector Network Analyzer (VNA) that generates a stepped frequency waveform (1 GHz bandwidth with 5 MHz step size). Horn antenna (1 GHz bandwidth) is used in mono-static mode for transmitting and receiving signals. Antenna is mounted on 2D-scanning frame which can slide along cross range and height. Scanning is precisely controlled by micro-controller and at each point scattering parameters are recorded by

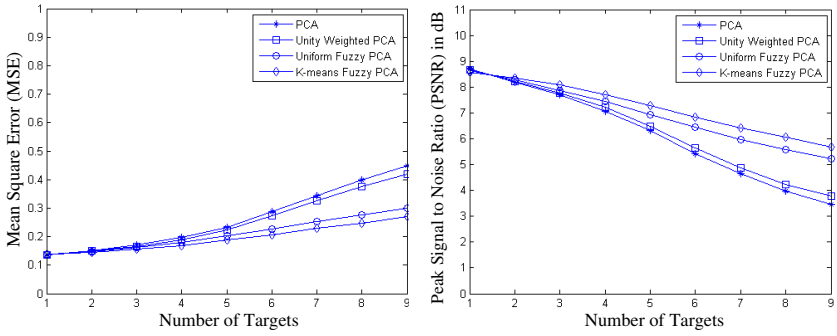

Figure 10. MSE and PSNR comparison of conventional PCA and proposed Fuzzy PCA against number of targets. (a) MSE comparison. (b) PSNR comparison.

VNA and transferred to local computer for image reconstruction and post processing tasks. Time delays and weights are fed into beamforming algorithm for image reconstruction. Image enhancement algorithms (PCA and proposed fuzzy logic based PCA) are simulated in MATLAB and results are compared on the basis of MSE, PSNR and visual inspection.

$$\text{MSE} = \frac{1}{M \times N} \sum_{n=1}^{N} \sum_{m=1}^{M} \left(F_{bs}(n,m) - F_{tar}(n,m)\right)^2$$

$$\text{PSNR(dB)} = 10 \log_{10} \frac{1}{\text{MSE}}$$

F_{bs} is background subtracted image used for comparison of proposed and existing algorithms. Figure 8 shows the performance of conventional PCA and proposed fuzzy PCA based schemes for single target. It can be seen that conventional and proposed schemes provide comparable results. Figure 9 shows that proposed method successfully detects all six targets (placed randomly behind wall) while conventional PCA algorithm is not able to detect. Figure 10 summarizes MSE and PSNR plots for different number of targets placed behind wall. For single target conventional PCA and proposed fuzzy PCA schemes give comparable results but as number of target increases proposed scheme perform significantly better (compare to conventional PCA).

4. CONCLUSION

Fuzzy logic and PCA based image enhancement technique capable of discriminating between target and clutter signals is proposed for TWI. The proposed scheme is capable of detecting single and multiple targets in heavy clutter environment. Moreover, assigning membership functions by K-means clustering results in better performance than uniform membership functions. Simulation results show that the proposed fuzzy logic based PCA based image enhancement scheme has significant improvement in conventional PCA based image enhancement. The proposed scheme can also be modified for other statistical methods such as SVD, FA, and ICA to get better accuracy.

REFERENCES

1. Baranoski, E., "Through-wall imaging: Historical perspective and future directions," *Journal of the Franklin Institute*, Vol. 345, No. 6, 556–569, 2008.
2. Ferris, D. D. and N. C. Currie, "A survey of current technologies for through the wall surveillance (TWS)," *Proceedings of the SPIE*, Vol. 3577, 62–72, 1998.
3. Muqaibel, A., A. Safaai-Jazi, A. Bayram, M. Attiya, and S. M. Riad, "Ultrawideband through-the-wall propagation," *IEE Proceedings Microwave, Antennas and Propagation*, Vol. 152, 581–588, 2005.
4. Amin, M. G., *Through the Wall Radar Imaging*, CRC press, USA, 2011.
5. Zheng, W., Z. Zhao, and Z. P. Nie, "Application of TRM in the UWB through wall radar," *Progress In Electromagnetics Research*, Vol. 87, 279–296, 2008.
6. Solimene, R., F. Soldovieri, G. Prisco, and R. Pierri, "Three-dimensional throughwall imaging under ambiguous wall parameters," *IEEE Transaction on Geo-science and Remote Sensing*, Vol. 47, No. 5, 1310–1317, 2009.
7. Zhu, F., S. C. Gao, A. T. S. Ho, T. W. C. Brown, J. Li, and J. D. Xu, "Low-profile directional ultra-wideband antenna for see-through-wall imaging applications," *Progress In Electromagnetics Research*, Vol. 121, 121–139, 2011.
8. Wang, G. and M. G. Amin, "Imaging through unknown walls using different standoff distances," *IEEE Transaction on Signal Processing*, Vol. 54, 4015–4025, 2006.

9. Lu, T., K. Agarwal, Y. Zhong, and X. Chen, "Through-wall imaging: Application of subspace-based optimization method," *Progress In Electromagnetics Research*, Vol. 102, 351–366, 2010.
10. Yang, Y., Y. Wang, and A. E. Fathy, "Design of compact Vivaldi antenna arrays for UWB see through wall applications," *Progress In Electromagnetics Research*, Vol. 82, 401–418, 2008.
11. Ahmad, F., M. G. Amin, and G. Mandapati, "Autofocusing of through-the-wall radar imagery under unknown wall characteristics," *IEEE Transactions on Image Processing*, Vol. 16, 1785–1795, 2007.
12. Jia, Y., L. Kong, and X. Yang, "A novel approach to target localization through unknown walls for through-the-wall radar imaging," *Progress In Electromagnetics Research*, Vol. 119, 107–132, 2011.
13. Aftanas, M., "Through-wall imaging with UWB radar system," Ph.D. Dissertation, Technical University of Kosice, 2009.
14. Moulton, J., S. A. Kassam, F. Ahmad, M. G. Amin, and K. Yemelyanov, "Target and change detection in synthetic aperture radar sensing of urban structures," *Proceedings IEEE Radar Conference*, 1–6, 2008.
15. Yoon, Y. S. and M. G. Amin, "Spatial filtering for wall clutter mitigation in through-the-wall radar imaging," *IEEE Transactions on Geosciences and Remote Sensing*, Vol. 47, 3192–3208, 2009.
16. Zhang, W., A. Hoorfar, and L. Li, "Through-the-wall target localization with time reversal music method," *Progress In Electromagnetics Research*, Vol. 106, 75–89, 2010.
17. Dehmollaian, M. and K. Sarabandi, "Refocusing through building walls using synthetic aperture radar," *IEEE Transactions on Geosciences and Remote Sensing*, Vol. 46, 1589–1599, 2008.
18. Smith, G. and B. G. Mobasseri, "Robust through-the-wall radar image classification using a target-model alignment procedure," *IEEE Transactions on Image Process.*, 2011.
19. Zheng, W., Z. Zhao, Z. P. Nie, and Q. H. Liu, "Evaluation of TRM in the complex through wall environment," *Progress In Electromagnetics Research*, Vol. 90, 235–254, 2009.
20. Tivive, F. H., M. G. Amin, and A. Bouzerdoum, "Wall clutter mitigation based on eigen analysis in through the wall radar imaging," *Digital Signal Processing*, 1–8, 2011.
21. Ram, S. S., C. Christianson, K. Youngwook, and L. Hao, "Simulation and analysis of human micro-dopplers in through-wall

environments," *IEEE Transaction on Geo-science and Remote Sensing*, Vol. 48, 2015–2023, 2010.

22. Debes, C., "Advances in detection and classification for through the wall radar imaging," Ph.D. Dissertation, Technische University Darmstadt, 2010.
23. Gaikwad, A. N., D. Singh, and M. J. Nigam, "Recognition of target in through wall imaging using shape feature extraction," *IEEE International Geosciences and Remote Sensing Symposium*, 957–960, 2011.
24. Chandra, R., A. N. Gaikwad, D. Singh, and M. J. Nigam, "An approach to remove the clutter and detect the target for ultra-wideband through-wall imaging," *Journal of Geophysics and Engineering*, 2008.
25. Wang, F.-F. and Y.-R. Zhang, "A real-time through-wall detection based on support vector machine," *Journal of Electromagnetic Waves and Applications*, Vol. 25, No. 1, 75–84, 2011.
26. Lee, K.-C., J.-S. Ou, and M.-C. Fang, "Application of SVD noise-reduction technique to PCA based radar target recognition," *Progress In Electromagnetics Research*, Vol. 81, 447–459, 2008.
27. Verma, P. K., A. N. Gaikwad, D. Singh, and M. J. Nigam, "Analysis of clutter reduction techniques for through wall imaging in UWB range," *Progress In Electromagnetics Research*, Vol. 17, 29–48, 2009.
28. Cois, J. C., "Blind signal separation: Statistical principles," *IEEE Proceedings*, Vol. 86, No. 10, 2009–2025, 1998.
29. Wall, M. E., A. Rechtsteiner, and L. M. Rocha, "Singular value decomposition and principal component analysis, a practical approach to microarray data analysis," 2003.
30. Yager, R. and D. Filev, *Essentials of Fuzzy Modeling and Control*, Wiley, USA, 1994.
31. Wang, L. X., *A course in Fuzzy Systems and Control*, Prentice Hall PTR, USA, 1997.
32. Kanungo, T., D. M. Mount, N. S. Netanyahu, C. D. Piatko, R. Silverman, and A. Y. Wu, "An efficient K-means clustering algorithm: Analysis and implementation," *IEEE Transactions Pattern Analysis and Machine Intelligence*, Vol. 24, 881–892, 2002.